Vol. A51 (1977) ACTA PHYSICA POLONICA No 2

BAND STRUCTURE CALCULATION AND FERMI SURFACE OF INDIUM-TIN ALLOYS*

By S. Maciejewski and M. Surma

Institute of Physics, A. Mickiewicz University, Poznań**

(Received May 22, 1976)

Applying the pseudopotential method, the electronic structure of In_3Sn alloys in β-phase is determined for 16.2, 20, 25.03, and 30% of Sn atomic concentration in the alloy. The calculations are based on the model pseudopotentials of Animalu and Heine for indium and tin which, for the unordered structure of the alloys analyzed, are used to calculate the pseudopotential of the mean crystallographical lattice. Numerical solutions of the band structure of the alloys are derived for the $\vec{k}$ values in the directions T–U, U–X, Γ–W, W–T, N–W determined by the symmetry points of the Brillouin zone and in the directions U–C, S–B and S–D additionally chosen in the Brillouin zone. The electronic structure of In_3Sn alloys is characterized by the presence in the third band of an electron cigar-shaped pocket of the Fermi surface.

1. Introduction

In recent years, the pseudopotential method has been successfully applied to the electronic structure analysis of metal alloys. The method has proved effective with regard to metals, for a number of which model pseudopotentials are at present available [1]. The latter have been applied, e. g., by Hughes and Shepherd [2] and Ashcroft and Lawrence [3] to determine the band structure of indium. The method is applicable as well in determinations of the electronic structure of metal alloys. Thus, it has been applied by Hughes, Shepherd and Gaulton [4] to dilute indium-tin and indium-lead alloys containing 0.17% of tin and 0.60% of lead, respectively. The authors [4] proved the necessity of introducing a pseudopotential dependent on the concentrations of the components. Even if the alloy is highly dilute, so that the concentration of one of its components does not exceed 0.17%, the "rigid model" fails to yield correct results unless the pseudopotential is not dealt with as a function of the concentrations of the components.

In this paper, we determine the electronic structure of indium-tin alloys (In_3Sn) in the β-phase. Our analysis bears on alloys of the concentrations: 16.2, 20, 25.03, and 30

* Work sponsored by the Polish Academy of Sciences under project 06.2.1-04.2.

** Address: Instytut Fizyki, Uniwersytet A. Mickiewicza, Grunwaldzka 6, 60-780 Poznań, Poland.

atom percent of tin applying the method of pseudopotential and taking into account the change of the latter, the change of the lattice constants[1], and the change of the Fermi energy E_F in their dependence on the tin concentration of the alloys.

2. The crystal lattice of indium-tin alloy in the β-phase

Indium-tin alloy in the β-phase possesses a pseudotetragonal lattice [5, 6]. This is a disordered alloy [7], and the probability of occupation of a given lattice node by an indium atom is proportional to the indium concentration of the alloy, whereas that of occupation of a node by a tin atom is proportional to the tin concentration. We refer to the set of these lattice nodes as the mean crystal lattice which, in the case of In_3Sn alloy, is a space centred tetragonal one. The values of the lattice constants of the alloy as functions of the atomic concentrations of the components are known from X-ray determinations [5, 8]. These data, as well as the disordered structure of the In_3Sn alloys, led us to the pseudopotential method of In_3Sn band structure determination, consisting in the following.

The pseudopotential matrix element for two arbitrary plane wave functions can be expressed [9] in the form

$$\langle \vec{k}+\vec{q}|\omega|\vec{k}\rangle = (1/N)\sum_{j(1)} e^{-i\vec{q}\cdot\vec{r}_j}\langle \vec{k}+\vec{q}|\omega_1|\vec{k}\rangle + (1/N)\sum_{j(2)} e^{-i\vec{q}\cdot\vec{r}_j}\langle \vec{k}+\vec{q}|\omega_2|\vec{k}\rangle. \tag{1}$$

In the first and second term of Eq. (1), summation extends respectively over nodes occupied by indium atoms **1** and tin atoms **2**. N denotes the number of all atoms; $\langle \vec{k}+\vec{q}|\omega_1|\vec{k}\rangle$ and $\langle \vec{k}+\vec{q}|\omega_2|\vec{k}\rangle$ are the pseudopotentials for indium and tin, respectively. For $\vec{q}$ taking values of the reciprocal lattice vectors

$$\vec{k}_n = n_1\vec{b}_1 + n_2\vec{b}_2 + n_3\vec{b}_3 \tag{2}$$

where

$$\vec{b}_1 = \frac{2\pi}{a}\vec{i} + \frac{2\pi}{a}\vec{j} - \frac{2\pi}{c}\vec{k},$$

$$\vec{b}_2 = \frac{2\pi}{a}\vec{i} - \frac{2\pi}{a}\vec{j} + \frac{2\pi}{c}\vec{k},$$

$$\vec{b}_3 = -\frac{2\pi}{a}\vec{i} + \frac{2\pi}{a}\vec{j} + \frac{2\pi}{c}\vec{k}, \tag{3}$$

and $n_1, n_2, n_3 = 0, \pm 1, \pm 2, \ldots$ constructed with the translation vectors for the mean lattice

$$\vec{a}_1 = \frac{a}{2}\vec{i} + \frac{a}{2}\vec{j}, \quad \vec{a}_2 = \frac{a}{2}\vec{i} + \frac{c}{2}\vec{k}, \quad \vec{a}_3 = \frac{a}{2}\vec{j} + \frac{c}{2}\vec{k},$$

[1] The authors wish to thank Dr R. Horyń, of the Institute of Low Temperature and Structure Research, Polish Academy of Sciences, Wrocław, for providing the lattice constants of the In_3Sn alloys studied.

the exponential terms $e^{-i\vec{q}\cdot\vec{r}_j}$ are unity. In the present case, the matrix element defined by Eq. (1) becomes

$$\langle\vec{k}+\vec{k}_n|\omega|\vec{k}\rangle = f_1\langle\vec{k}+\vec{k}_n|\omega_1|\vec{k}\rangle+f_2\langle\vec{k}+\vec{k}_n|\omega_2|\vec{k}\rangle. \tag{4}$$

The quantities f_1 and f_2 define, respectively, the concentration of indium and tin atoms in the alloy.

For $\vec{q}$ equal to the reciprocal lattice vector $\vec{k}_n$, the matrix element given by Eq. (4) is independent of the distribution of the various kinds of atoms in the lattice nodes.

In order to determine the value of the matrix element (Eq. (1)) for $\vec{q}$ different from $\vec{k}_n$, we transform Eq. (1) to the following form:

$$\langle\vec{k}+\vec{q}|\omega|\vec{k}\rangle = 1/N\sum_j e^{-i\vec{q}\cdot\vec{r}_j}\langle\vec{k}+\vec{q}|\omega_1|\vec{k}\rangle+1/N\sum_{j(2)} e^{-i\vec{q}\cdot\vec{r}_j}\langle\vec{k}+\vec{q}|\omega_2-\omega_1|\vec{k}\rangle. \tag{5}$$

Summation in the first term of Eq. (5) extends over all nodes of the mean lattice and the structural factor occuring in this term

$$1/N\sum_j e^{-i\vec{q}\cdot\vec{r}_j} = S(\vec{q}), \tag{6}$$

vanishes for $\vec{q}\neq\vec{k}_n$. Hence, Eq. (5) reduces to the form

$$\langle\vec{k}+\vec{q}|\omega|\vec{k}\rangle = S_2(\vec{q})\,\langle\vec{k}+\vec{q}|\omega_2-\omega_1|\vec{k}\rangle \tag{7}$$

where $S_2(\vec{q})$, for completely random distribution of the component atoms in the nodes of the alloy [9], fulfils the relation

$$|S_2(q)|^2 = \frac{f_1 f_2}{N}. \tag{8}$$

Comparison of the expressions of Eqs (4), (7) and (8) shows that the pseudopotential matrix element for $\vec{q}$ equal to the reciprocal lattice vector $\vec{k}_n$ possesses a value strongly in excess of the absolute value of the matrix element for arbitrary $\vec{q}$. The foregoing fact justifies our approach to In_3Sn alloy, when calculating its band structure, as a crystal having an ideal crystal lattice with one atom in the elementary cell and the pseudopotential [2] calculated from Eq. (4).

3. The band structure of In_3Sn alloy

We calculated the band structure of In_3Sn alloys of the concentrations given in Table I by applying the pseudopotential method [9–12] and having recourse to the pseudopotentials given by Animalu and Heine [1, 13]. For each of the alloys of Table I, we calculated the Fermi energy in the free electron approximation using the well known relation [4]

$$E_F = \frac{\hbar^2}{2m}\left[\frac{3(3f_1+4f_2)V_B}{8\pi}\right]^{2/3} \tag{9}$$

TABLE I

Fermi energy E_F and a/c lattice constant ratio for In_3Sn alloys

Concentration % at. Sn	$E_F[R_y]$	a/c
16.2	0.6548	1.095
20	0.6592	1.107
25.03	0.6656	1.119
30	0.6717	1.126

where V_B is the volume of the first Brillouin zone, equal to

$$V_B = 4\frac{(2\pi)^3}{a^2c}, \tag{10}$$

and a, c are the lattice constants of the alloy. The Fermi energies E_F, calculated from Eqs (9) and (10) are given numerically in Table I. Applying the reciprocal lattice vectors defined by Eq. (2), we also determined the first Brillouin zone of the alloys; its shape is

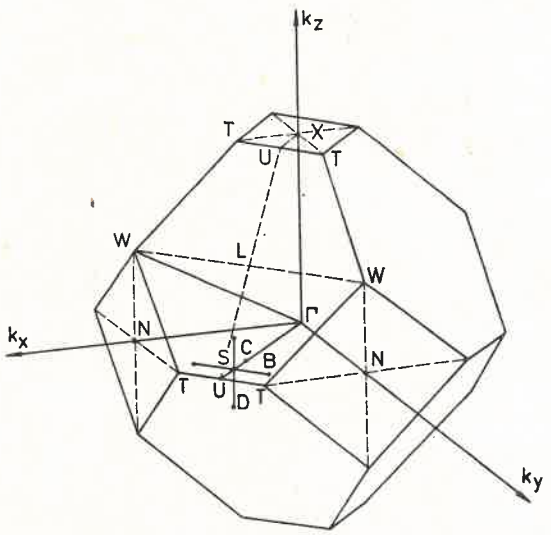

Fig. 1. Brillouin zone for In_3Sn alloy

shown in Fig. 1 and its dimensions for 25.03% alloy are given in Table II. In alloys with a tin concentration upwards of 25.03% the Brillouin zone undergoes a slight elongation in the direction of the k_z–axis. For tin concentrations lower than 25.03%, it undergoes a slight shortening in the same direction. For a quantitative illustration, see the a/c ratios of Table I.

TABLE II

Dimensions of Brillouin zone for In_3Sn alloy of concentration 25.03% at. Sn

Symmetry point of Brillouin zone	$k_x[Å^{-1}]$	$k_y[Å^{-1}]$	$k_z[Å^{-1}]$
Γ	0	0	0
N	1.280	0	0
X	0	0	1.433
W	1.280	0	0.716
T	1.280	0.800	0
T	0.475	0	1.433
U	0.238	0.238	1.433
U	1.042	1.042	0
S	0.998	0.998	0
C	0.969	0.969	0
D	0.998	0.998	0.104

The determination of the band structure of the alloys reduces to solving the following secular equation

$$\det |[T_n(\vec{k}, E_k) - E_n(\vec{k})]\delta_{nl} + \langle \vec{k}+\vec{k}_n|\overline{W}|\vec{k}+\vec{k}_l\rangle| = 0 \tag{11}$$

where

$$T_n(\vec{k}, E_k) = \frac{\hbar^2}{2m}(\vec{k}+\vec{k}_n)^2.$$

We calculated the nondiagonal matrix elements of the preceding equation by having recourse to the relation [14]

$$\langle \vec{k}+\vec{k}_n|\overline{W}|\vec{k}+\vec{k}_l\rangle = f_1\langle \vec{k}+\vec{k}_n|\omega_1|\vec{k}+\vec{k}_l\rangle + f_2\langle \vec{k}+\vec{k}_n|\omega_2|\vec{k}+\vec{k}_l\rangle$$

$$+ \sum_{\vec{k}_m} \frac{(f_1\langle \vec{k}+\vec{k}_n|\omega_1|\vec{k}+\vec{k}_m\rangle + f_2\langle \vec{k}+\vec{k}_n|\omega_2|\vec{k}+\vec{k}_m\rangle)(f_1\langle \vec{k}+\vec{k}_m|\omega_1|\vec{k}+\vec{k}_l\rangle + f_2\langle \vec{k}+\vec{k}_m|\omega_2|\vec{k}+\vec{k}_l\rangle)}{\frac{\hbar^2}{2m}[\vec{k}_0^2 - (\vec{k}_0+\vec{k}_m)^2]} \tag{12}$$

Numerically, the matrix elements $\langle \vec{k}+\vec{k}_n|\omega_1|\vec{k}\rangle$ and $\langle \vec{k}+\vec{k}_n|\omega_2|\vec{k}\rangle$ occurring in the right hand term of Eq. (12) were calculated using the data tabulated by Animalu and Heine [1] giving the matrix element values in the local pseudopotential approximation.

The vectors $\vec{k}_n$ and $\vec{k}_l$ in Eq. (12) take the following values for the successive rows and columns of the determinant occuring in Eq. (11)

$$\begin{aligned} \vec{k}_1 &= 0, & \vec{k}_4 &= -\vec{b}_1 - \vec{b}_2 - \vec{b}_3, \\ \vec{k}_2 &= -\vec{b}_1, & \vec{k}_5 &= -\vec{b}_1 - \vec{b}_2, \\ \vec{k}_3 &= -\vec{b}_2, & \vec{k}_6 &= -\vec{b}_2 - \vec{b}_3. \end{aligned} \tag{13}$$

In Eq. (12), summation of terms over indices m was performed for the reciprocal lattice vectors

$$\vec{k}_m = m_1\vec{b}_1 + m_2\vec{b}_2 + m_3\vec{b}_3$$

for values of m from the intervals

$$-E \leqslant m_1 \leqslant E, \quad -E \leqslant m_2 \leqslant E, \quad -E \leqslant m_3 \leqslant E, \tag{14}$$

where E is an integer. The foregoing summation does not comprise reciprocal lattice vectors defined by Eq. (13). This ensures that the description of the band structure shall take into account the contribution from pseudopotential matrix elements constructed with reciprocal lattice vectors not contained in the set defined by Eq. (13) but occurring in the interval of m-values of Eq. (14).

The vector $\vec{k}_0$ of Eq. (12) has a constant value close to that of the wave vector $\vec{k}$, as functions of which the dispersion relations $E(\vec{k})$ are calculated.

The secular equation was solved by Odra 1204 computer, calculating the dispersion relations $E(\vec{k})$ for In_3Sn alloys with 16.2, 20, 25.03, and 30% atomic concentration of tin.

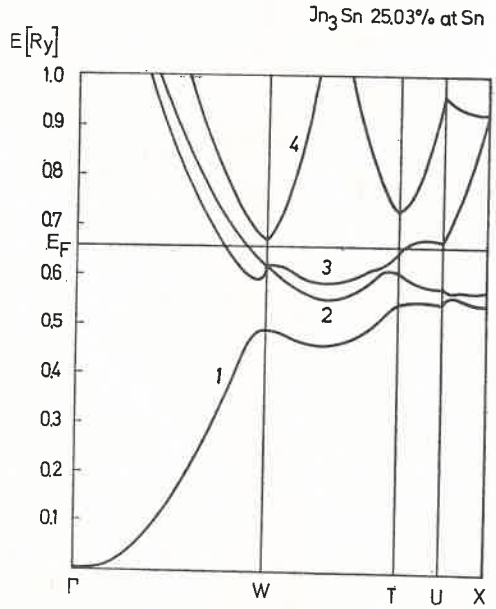

Fig. 2. Band structure of In_3Sn alloy in the symmetry directions Γ–W, W–T, T–U and U–X

In the directions $T-U$, $U-X$ of the Brillouin zone shown in Fig. 1, we assumed for the vector $\vec{k}_0$ the coordinates of the point U and the value $E = 3$. For the directions $\Gamma-W$, $W-T$, $N-W$, our calculations were performed assuming for $\vec{k}_0$ the coordinates of the point W and $E = 3$. For the directions $T-U$, $U-C$, $S-B$ and $S-D$, we assumed for $\vec{k}_0$

the coordinates of the point U but $E = 4$. This procedure provides sufficiently good information about the relation $E(\vec{k})$ in the selected symmetry directions.

The dispersion relations thus derived are shown in Figs 2, 3 and 4. Fig. 2 shows solely the results for 25.03% tin concentration. The dispersion relations $E(\vec{k})$ shown in Fig. 2 provide a good illustration of the graphs describing the bands in the other In_3Sn alloys studied [8], i.e. in those containing 16.2, 20, and 30% atomic concentration of tin.

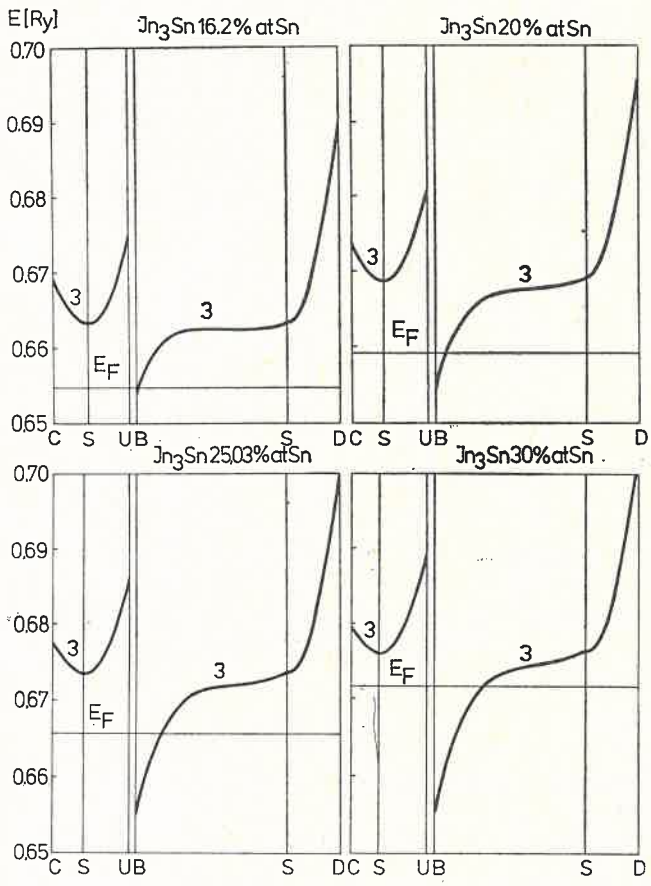

Fig. 3. Third band in In_3Sn alloys close to the symmetry point S

The number of directions between symmetry points along which $E(\vec{k})$ was determined in this investigation is not complete. Only $E(\vec{k})$ relationships between symmetry points yielding essential information on the band shape and the principal elements of the Fermi surface topography are considered. The results shown in Figs 3 and 4 which, supplementing the dispersional data of the bands (Fig. 2), provide a basis for the formulation of conclusions regarding the Fermi surface of the alloys, serve the same purpose.

In order to gain quantitative information concerning the spin-orbit interaction energy and its influence on the position of the bands, we calculated it for band 4 in the symmetry

point W of the Brillouin zone. The results of these calculations show [8] that the effect of spin-orbit interactions is insignificant. Hence we draw the conclusion that spin-orbit interactions fail to affect significantly the $E(\vec{k})$ dispersion relations along the symmetry directions of the Brillouin zone analyzed.

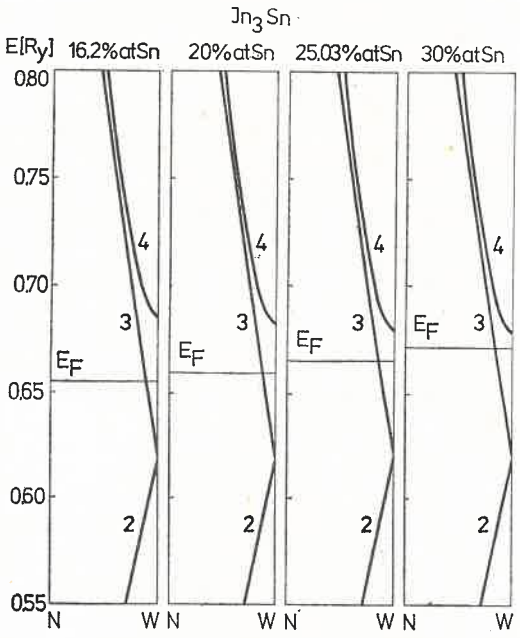

Fig. 4. Dispersion relations for the second, third and fourth band close to the symmetry point W of the Brillouin zone for In_3Sn alloys

4. *Conclusions*

From the dispersion relations of Figs 2, 3 and 4 and the Fermi energy values E_F calculated (Table I), the shape of the Fermi surface of the In_3Sn alloys considered can be characterized qualitatively as follows: The first band **1** is completely occupied and does not contribute to the Fermi surface of the alloy. The second band **2**, which is partly occupied, is responsible for the existence of a closed sphere of holes. This sphere is disposed centrally in the Brillouin zone, and decreases in size with increasing tin concentration of the alloy.

The Fermi sphere of electrons in the third band **3** consists of cigar-shaped surfaces (Fig. 5). The size of the sphere increases with increasing tin concentration. The gap between the bottom of the unoccupied part of the band situated in the point S of the Brillouin zone and the Fermi level E_F decreases slightly at higher tin concentrations. The effect is well apparent in Fig. 3.

The fourth band **4** of the Brillouin zone is unoccupied, and does not contribute to the Fermi surface. It lies closest to the Fermi level E_F in the symmetry point W of the

Brillouin zone; the energy gap between its bottom and the Fermi level decreases with increasing tin concentration, as shown in Fig. 4. Linear extrapolation of the gap between the band and the Fermi level as a function of the tin concentration leads to the conclusion that, at 32% tin content, In_3Sn alloy should exhibit a zero energy gap between E_F and the level of the fourth band in the point W of the Brillouin zone.

From the above considerations, the Fermi surface of In_3Sn alloy is found to resemble, in numerous topographical elements, the Fermi surface of indium. The data for indium

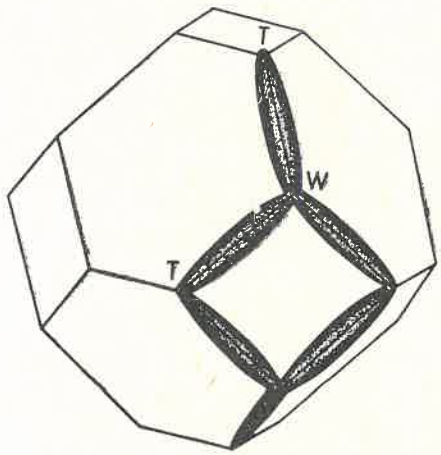

Fig. 5. Electron Fermi surface of the third band for In_3Sn alloy

are to be found in Refs [2–4]. Both in pure indium and In_3Sn alloys, the first band is completely occupied, the second band forms a closed sphere of holes, whereas the fourth band is unoccupied. Pure indium, like the In_3Sn alloys analyzed by us, has a tetragonal crystal lattice.

The essential difference between the band structure of indium and In_3Sn resides in the Fermi surface, which forms the third band. In In_3Sn, this pocket of the Fermi surface (Fig. 5) consists of electron cigars disposed allong the symmetry directions $T-W$ of the Brillouin zone, whereas in the case of indium the cigars lie in directions $T-T$ [2].

REFERENCES

[1] A. O. E. Animalu, V. Heine, *Phil. Mag.* **12**, 1249 (1965).
[2] A. I. Hughes, J. P. G. Shepherd, *J. Phys.* **C2**, 661 (1969).
[3] N. W. Ashcroft, W. E. Lawrence, *Phys. Rev.* **175**, 938 (1968).
[4] A. I. Hughes, I. P. G. Shepherd, D. F. Gaulton, *J. Phys.* **C3**, 2461 (1970).
[5] W. B. Pearson, *A Handbook of Lattice Spacings and Structures of Metals and Alloys*, Pergamon Press 1967.
[6] R. M. Screaton, R. B. Ferguson, *Acta Cryst.* **7**, 364 (1954).
[7] R. Kubiak, K. Łukaszewicz, *Bull. Acad. Pol. Sci. Sér. Sci. Chim.* **22**, 281 (1974).
[8] S. Maciejewski, *Phys. Status Solidi* b **66**, 633 (1974).

[9] W. A. Harrison, *Pseudopotentials in the Theory of Metals*, W. A. Benjamin, Inc., New York–Amsterdam 1966.
[10] J. C. Phillips, L. Kleinman, *Phys. Rev.* **116**, 287, 880 (1959).
[11] V. Heine, *Proc. R. Soc.* **240**, 361 (1957).
[12] M. H. Cohen, V. Heine, *Phys. Rev.* **122**, 1821 (1961).
[13] V. Heine, I. Abarenkov, *Phil. Mag.* **9**, 451 (1964).
[14] D. Brust, *Phys. Rev.* **134A**, 1337 (1964).